Design and Analysis of Orthogonally Compliant Features for Local Contact Pressure Relief in Transtibial Prostheses

Mario C. Faustini

Richard H. Crawford
e-mail: rhc@mail.utexas.edu

Richard R. Neptune

Department of Mechanical Engineering,
The University of Texas at Austin,
Austin, Texas 78712

William E. Rogers

Gordon Bosker

Department of Rehabilitation Medicine,
The University of Texas Health Science
Center at San Antonio,
San Antonio, Texas 78229

A very attractive advantage of manufacturing prosthetic sockets using solid freeform fabrication is the freedom to introduce design solutions that would be difficult to implement using traditional manufacturing techniques. Such is the case with compliant features embedded in amputee prosthetic sockets to relieve contact pressure at the residual limb-socket interface. The purpose of this study was to present a framework for designing compliant features to be incorporated into transtibial sockets and manufacturing prototypes using selective laser sintering (SLS) and Duraform™ material. The design process included identifying optimal compliant features using topology optimization algorithms and integrating these features within the geometry of the socket model. Using this process, a compliant feature consisting of spiral beams and a supporting external structure was identified. To assess its effectiveness in reducing residual limb-socket interface pressure, a case study was conducted using SLS manufactured prototypes to quantify the difference in interface pressure while a patient walked at his self-selected pace with one noncompliant and two different compliant sockets. The pressure measurements were performed using thin pressure transducers located at the distal tibia and fibula head. The measurements revealed that the socket with the greatest compliance reduced the average and peak pressure by 22% and 45% at the anterior side distal tibia, respectively, and 19% and 23% at the lateral side of the fibula head, respectively. These results indicate that the integration of compliant features within the socket structure is an effective way to reduce potentially harmful contact pressure and increase patient comfort.
[DOI: 10.1115/1.2049331]

Introduction

In many applications involving mechanical structures, compliance is a fundamental characteristic for optimal part functionality. In other applications, compliance is not essential but provides an elegant and functional design solution where, for instance, joints and links of mechanisms can be replaced by the incorporation of controlled flexibility within the structure itself. However, the design of compliant features is very challenging as well defined constraints need to be considered and evaluated in order to successfully implement such features [1]. These design constraints include accounting for the part material and mechanical properties, defining appropriate boundary conditions, identifying the target deformation under specific loads, and assessing the feature's structural integrity through engineering analysis.

This article focuses on the design of orthogonally compliant features where the load-displacement direction is normal to the structure surface, and the integration of these features in the context of relieving residual limb-socket interface contact pressure in transtibial amputee prosthetic sockets. The identified solutions were implemented in socket prototypes manufactured using selective laser sintering (SLS), a versatile layer-based manufacturing process [2]. In SLS, a roller spreads a thermoplastic powder over the surface of a build cylinder. A high-powered laser is then traced over the surface of the thermoplastic powder to selectively sinter or melt the powder to form a layer of the object. Each trace is generated directly from a computer geometric model of the part. The piston in the build cylinder then moves down one object layer thickness to accommodate a new layer of powder. The process is repeated until the entire object is fabricated. Once the object is fully formed and cooled, unsintered powder is simply brushed away and the part is ready to be used.

The production of prosthetic sockets using SLS (e.g., Fig. 1) has several advantages over standard, more labor-intensive fabrication methods [3]. The main advantage is that SLS directly creates sockets from digital shape information, thus eliminating the need for intermediate molds, hand lamination and finishing procedures. Another advantage of SLS is the ability to create complex geometries with minimal cost penalty in manufacturing, which significantly expands the options for developing and exploring alternate socket designs.

In a socket design/SLS fabrication framework, a computer model of the socket is created from laser digitization of the patient's residual limb. In the present study, we were interested in using the general patellar tendon bearing (PTB) socket design, which is intended to load specific regions of the limb that can safely withstand the contact pressures generated during normal gait and support most of the limb-socket interface loads [4]. Although the patellar tendon region is well suited to handle high contact pressure, other regions of the residual limb are not. At these regions, high contact pressure can lead to patient discomfort during gait and affect patient recovery and rehabilitation, and in some cases pose a health risk for the patient [5,6]. Thus, it is essential to develop means to relieve contact pressure in selected regions while preserving an overall tight fit between the socket and residual limb. One promising solution is to make the socket wall orthogonally compliant at these high contact pressure regions.

Our previous approach for providing local compliance was to reduce the socket wall thickness at pressure sensitive areas (Fig.

Contributed by the Bioengineering Division for publication in the JOURNAL OF BIOMECHANICAL ENGINEERING. Manuscript received by the Bioengineering Division April 2, 2005; revision received July 7, 2005. Associate Editor: Teaching Cui.

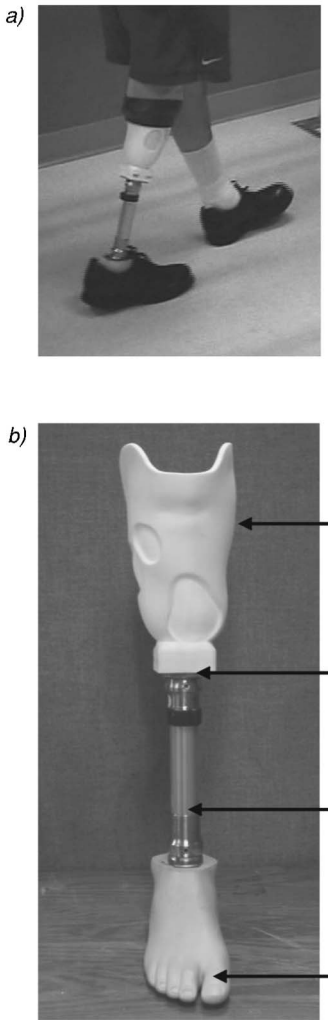

Fig. 1 (*a*) A patient using an SLS fabricated socket; (*b*) description of the parts of a prosthesis for below-the-knee amputees: (i) socket, (ii) attachment fitting, (iii) pylon, and (iv) prosthetic foot

1). However, this approach provided limited compliance and pressure relief [4]. More effective designs are possible by taking advantage of the ability of SLS to easily create geometric variants of traditional socket shapes to allow locally controlled expansion of the socket volume through deformation of the socket wall at sites where pressure relief is critical. The objective of the present study was to explore such designs.

Methods

Overview. The method used for designing and implementing orthogonally compliant features for prosthetic sockets initially involved identifying the design constraints and boundary conditions and the material characteristics used in the SLS fabrication process. A preliminary study identified several variants of compliant features that were analyzed and tested through experimentation to identify those that provided the greatest compliance. These features were combined with structures developed using a topology optimization algorithm to precisely control the compliance. The resulting compliant features were then incorporated into a nominal PTB socket design and fabricated using SLS. To assess the effectiveness of the design, a case study was performed on a patient using three SLS fabricated sockets (all were topologically similar, two with different levels of compliance and one without) and

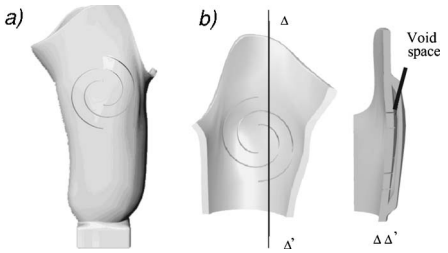

Fig. 2 (*a*) Example of orthogonally compliant spiral-slotted features incorporated in a socket; (*b*) a detailed view of spiral slot compliant feature and a section view showing the void space between the slotted wall and the back protective wall

quantifying the resulting changes in interface pressure at the compliant sites using thin pressure sensors. Below, details of the design and analysis are described.

Design Constraints. In order to design orthogonally compliant features to be incorporated into the socket structure, the target deformation for the compliant region when subjected to the pressure distribution experienced during normal walking needed to be specified. However, identifying an optimum value of the target displacement at the center of the compliant region is difficult to achieve, as it depends on several parameters that vary from patient to patient (e.g., condition of the limb, pain tolerance, geometry of the tissue and underlying bones) and subjective input from the prosthetist. To provide target displacement values in the present study, the socket/limb interface contact pressures at sensitive sites on the limb were experimentally measured in a gait lab using a non-compliant conventional socket [4,7]. These sensitive sites were identified by a certified prosthetist based on a clinical evaluation of the patient. From the pressure measurements and clinical examination, the prosthetist identified target displacement values.

Other important design constraints include (1) maintaining the structural integrity of the compliant features and socket during various loading conditions; (2) preserving the overall shape of the inside of the socket, which should follow as closely as possible the residual limb shape during deformation, thus reducing the occurrence of concentrated limb-socket contact pressures; (3) keeping the socket's outer profile close to that of a natural leg, a subjective criterion but important to many patients [6]; (4) minimizing the area of the compliant region defined by the prosthetist to maintain a tight overall fit; (5) minimizing void areas on the socket wall (e.g., slots and holes) to avoid high localized contact pressure gradients and concentrations that can create circulatory problems for the patient; and (6) preventing exposed spikes or sharp corners when compliant features are deformed, which can occur when slots in the socket wall self-intersect.

Design of Spiral Slot Compliant Features. A preliminary study [4] showed that compliant features including concentric spiral slots [Fig. 2(*a*)] was the best approach for relieving interface pressure at the residual limb-socket interface based on its capacity to provide orthogonal compliance in a relatively small area while satisfying the overall design constraints. However, through finite element method (FEM) analysis and experimental validation, the preliminary study also demonstrated that the optimum number of concentric slots (four) that provided a smooth deformation of the inner surface while preserving the structural integrity also led to an overshoot of the target compliance. The compliant feature was shown to provide little reaction force for a given displacement, which could potentially lead to a concentration of limb-socket contact pressures in the area around the compliant feature and result in poor socket fit. To remedy this situation, a stiffening structure was deemed necessary in order to provide increased stiffness and control compliance. Such a structure could be placed between the outer protective wall and the compliant feature [Fig.

2(*b*)]. However, it was unclear what form the stiffening structure should take. To identify potential structure designs, topology optimization was used, which is an ideal technique given the well-defined design domain and the freedom of design provided by the SLS fabrication process.

Topology Optimization of Features for Controlled Compliance. The topology optimization method used in this study was the homogenization method [8–10], specifically the solid isotropic material with penalization or "power-law" approach, where material properties are assumed to be constant within each element of the discretized design domain. This method involves the use of a material model that is physically feasible as long as the following condition is satisfied for the power p in a 2D design domain [11]:

$$p \geqslant p^*(\upsilon) = \max\left\{\frac{2}{1-\upsilon}, \frac{4}{1+\upsilon}\right\} \tag{1}$$

where υ is the value of Poisson's ratio.

The goal of the topology optimization was to design a structure that provided increased stiffness to limit the deflection of the spiral slot feature (i.e., minimize the compliance c of the structure). Hence, the objective function for the problem was formulated as

$$\text{min: } c([x]) = [d]^T[K] \cdot [d]$$

subject to

$$[K] \cdot [d] = [f]$$

$$V \leqslant V^* \tag{2}$$

$$[0] < [x]_{\min} \leqslant [x] \leqslant [1]$$

where $[d]$ is the displacement vector, $[f]$ is the force vector, $[K]$ is the stiffness matrix, V is the volume of material in design domain Γ, V^* is the total volume of design domain Γ, and $[x]$ is the design variable vector. In this case $[x]$ stores the densities of the elements, where

$$\varepsilon \leqslant x_i \leqslant 1$$

and ε is a positive minimum value (to avoid singularities).

The definition of the design domain was simplified to a 2D domain due to the approximate radial symmetry of the compliant feature [e.g., Fig. 3(*a*)]. Thus, based on symmetry (through the central vertical plane), the problem was locally defined by the design domain Γ [see Fig. 3(*b*)]. The rounded corner of the grey area [Fig. 3(*b*)] was defined to ensure smoothness of the structure with respect to the fixed socket geometry.

The objective function was thus rewritten in terms of the sum of the individual compliances of each four-noded finite element of the discretized design domain [see Fig. 3(*b*)] following the power-law approach:

$$c([x]) = \sum_{elements} (x_{element})^p [d]_{element}^T [K]_{element} [d]_{element} \tag{3}$$

where p is the penalization power.

To ensure convergence of the optimization problem, the design domain was constrained with appropriate boundary conditions to replicate the actual loading pattern and constraints that the compliant feature would be subjected to under working conditions [Fig. 3(*b*)]. Filtering techniques were applied to resolve two numerical problems: (1) the occurrence of checkerboard patterns in the solution due to the artificially high stiffness of such patterns when compared to uniform material distributions; and (2) the mesh dependency of the solution, which arises from differences in discretization. These problems were alleviated with the application of an appropriate convolution operator to the element sensitivities $\partial c / \partial x_{element}$ [12].

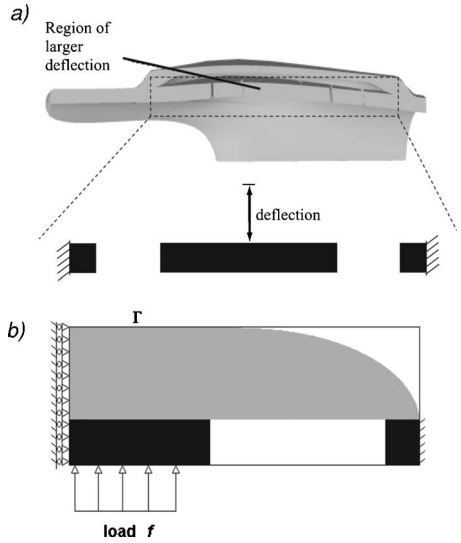

Fig. 3 (*a*) Section view of the spiral-slotted compliant feature [Fig. 2(*b*)] and corresponding schematic model of this section of the socket wall passing through the spiral-slotted feature. Note, an orthogonal deflection of center portion is desired while the border is fixed. (*b*) Definition of the design domain Γ, derived from symmetry through the central vertical plane of *a*. For the topology optimization problem, material presence is mandatory in the black areas, while material is not allowed in white areas, and gray areas indicate the sections to be optimized.

Sigmund [13] presented a MATLAB[1] program to solve a problem with basic boundary conditions (single constraint) using the optimality criteria. To allow for its use with multiple constraints, the optimizer was modified to include the method of moving asymptotes [14]. Also, a geometric finite element mesh representing the problem posed above [Fig. 3(*b*)] was created, with modified elements to ensure a fixed base structure and a desired degree of smoothness in the solution that would allow the design to be directly integrated into the socket. Several target compliances of the optimized feature were identified by altering the input value of the volume fraction V/V^*, which defines the amount of material available in the design domain to be topologically optimized. This produced structures with decreased compliance for larger volume fractions.

Integration of the Optimal Compliant Feature Into the Socket. The resulting compliant structure from the topology optimization was then incorporated into the socket design. This was performed by spatially revolving the resulting structure on top of the spiral-slotted compliant area around an axis passing through the center of the concentric spiral slots. This allowed us to take advantage of the radial symmetry of the slotted features. Inclusion of the compliant structure in the socket geometry was performed with a sequence of CAD operations involving trimming, stitching and Boolean operations using Rhinoceros[2] that provided a smooth transition between the compliant feature and the outer surface (Fig. 4).

Case Study: Pressure Measurements of Compliant Socket Prototypes. To experimentally evaluate the effectiveness of the resulting compliant features to reduce contact pressure, a case study was performed to compare pressure measurements recorded from three prototype SLS sockets with the same overall topology:

[1]MathWorks, Natick, MA.
[2]Robert McNeel & Associates, Seattle, WA.

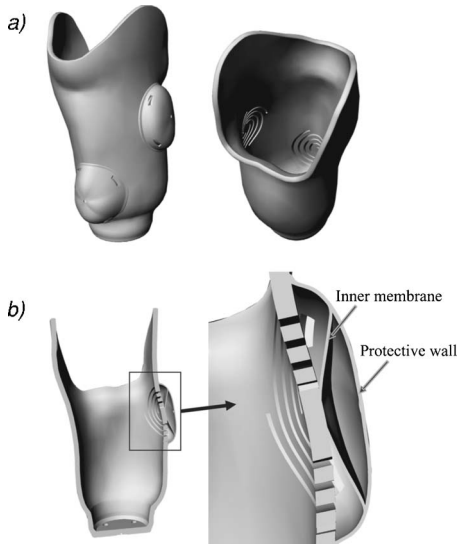

Fig. 4 (*a*) Views of a prosthetic socket with complete compliant features incorporated; (*b*) Section view of socket exposing the compliant features and detailed view of compliant feature

one socket had no compliant features while the other two incorporated the optimized compliant features at both the distal tibia and fibula head with different levels of compliance for each socket. One socket was 25% more compliant than the other. The overall wall thickness of each socket was 5 mm, the protective walls around the compliant features were 1 mm thick, and the gaps of the spiral slots were 2 mm wide. For the two compliant sockets, the membrane-like structure in the compliant features between the socket wall and the protective wall [Fig. 4(*b*)] had different values of thickness: 0.53 mm for the more compliant one and 0.68 mm for the less compliant one.

The material utilized in the SLS socket fabrication was DuraForm™ Polyamide (PA). This material is a type of nylon-12 processed into powder form by 3D Systems.[3] The CAD models of the sockets were exported using the STL (or stereolithography) format and prototypes were produced using a 3D Systems Sinterstation® Vanguard™. The models were fabricated in the vertical position for optimal sintering and thermal conditions, and were all built in the same run of the Sinterstation®. The total fabrication time, including the warm up and cool down phases, was 15 h, during which the machine operated completely unassisted. Once the fabrication was finished, the sockets were assembled into ready-to-wear prostheses.

Pressures at the tibia and fibula were measured using two F-Socket 9811 (Tekscan[4]) transducers. One transducer was trimmed to fit on the lateral side of the residual limb over the fibula head, while a second transducer was trimmed to cover the distal tibia on the anterior side of the residual limb. The trimmed transducers were then calibrated with a pressurized bladder calibration device at 345 kPa. Each transducer had dimensions of 76.2 mm $\times$ 203.2 mm, with a thickness of 0.28 mm, and consisted of 96 sensors (each with an area of 161.3 mm^2) arranged in 6 columns and 16 rows that provided a pressure range between 0 and 517 kPa. A portable data logger (F-Scan Mobile) was worn by the patient to record the pressure data at 60 Hz. The patient was an active male patient (age: 53 years; height: 1.80 m; mass: 93 kg) who had been a diabetic amputee for 3 years and was currently free from pain and discomfort in both limbs.

To maintain the sensor array position on the residual limb between different socket measurements, a sheet of thin heat shrink plastic was wrapped around the residual limb, allowing a 2.5 cm overlap. A medical spray adhesive was used to secure the plastic to the residual limb and the 2.5 cm overlapped area was glued to itself with contact cement. The plastic was gently warmed with a heat gun so that it conformed to the shape of the residual limb. The transducers were glued to the plastic around the residual limb [Fig. 5(*a*)], and positioned in order to occupy the contact area with the compliant features of the sockets [Fig. 5(*b*)]. This made it possible to change sockets without shifting the transducer positions.

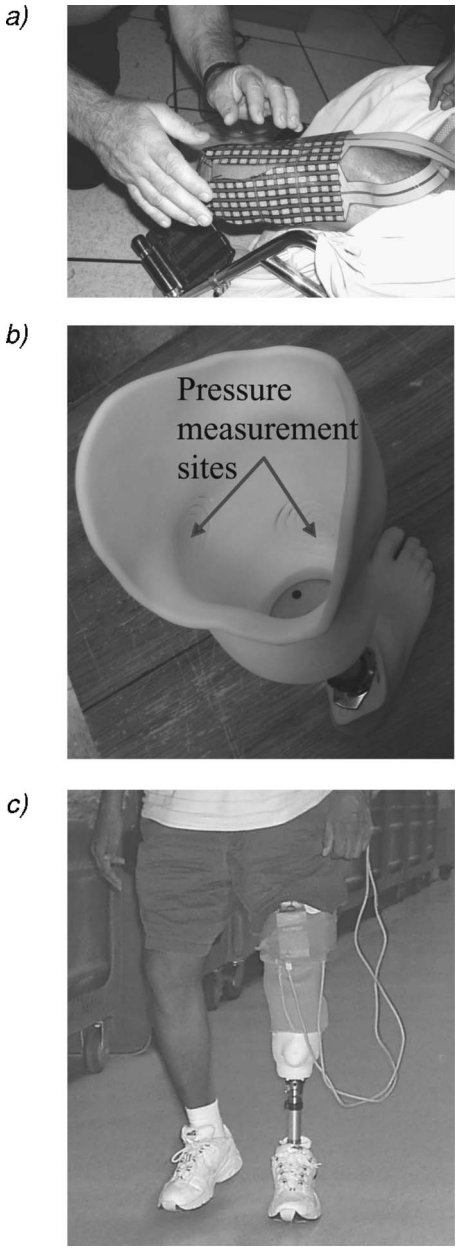

Fig. 5 (*a*) Pressure transducers fixed on the patient's residual limb at the fibula head and tibial area, (*b*) compliant socket with corresponding pressure measurement sites indicated, and (*c*) patient walking using socket with compliant features while limb-socket interface pressure data were collected with a portable data acquisition system.

The patient then put on the noncompliant socket and walked around the gait lab to verify the presence of the sensors did not hinder his normal walking motion. The patient performed two trials of straight-line walking at his self-selected pace while pres-

[3]Valencia, CA.
[4]South Boston, MA.

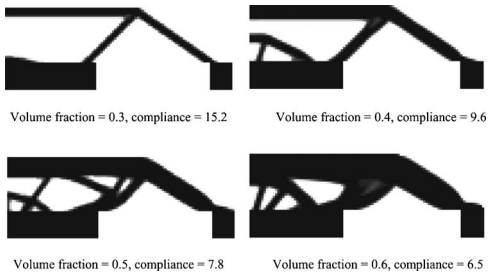

Fig. 6 Results of the topology optimization for an orthogonally compliant test disk for different input volume fractions and their theoretical compliances [as defined in Eq. (3)].

sure data was recorded for 30 s [Fig. 5(*c*)]. Then the patient put on each compliant socket and the procedure was repeated. F-Scan software (Tekscan) was used to calibrate the sensors before the test, download the data from the portable data logger after each test and visualize the results. The patient did not know *a priori* which one was the non-compliant socket and which one had compliant features until after the test, as they both contained spiral slots, but one was constrained to prevent displacement. The average and peak pressures during the single support phase of stance were calculated for each step cycle and averaged across steps for each socket (approximately 40 step cycles).

Results

Topology Optimization of Features for Controlled Compliance. The implemented topology optimization algorithms functioned as expected, generating increasingly stiffer structures for increasing input values for the initial volume fraction V/V^* (Fig. 6). The resulting structures were all feasible for manufacture with SLS. We chose to use the simplest resulting topology (Fig. 6, generated within the volume fraction range $V/V^* < 0.33$) as the final design to be integrated within the socket and manufactured using SLS.

Pressure Measurements. Analysis of the contact pressure measurements revealed that the most compliant socket reduced the average interface pressure at the distal tibia during the single support phase of stance by 22%, decreasing it from 67.51±17.23 kPa to 52.67±3.28 kPa relative to the socket with no compliant features (Table 1). The average peak pressure at the same site was reduced 45%, decreasing it from 103.35±15.59 kPa to 57.01±1.87 kPa [Fig. 7(*a*)].

The transducer at the fibula head revealed that the most compliant socket reduced the average interface pressure 19%, decreasing it from 73.85±9.03 kPa to 59.50±4.06 kPa, while the average peak pressure at the same site was reduced 23%, decreasing it from 82.74±1.84 kPa to 63.60±2.63 kPa [Fig. 7(*b*)]. After the walking tests, the patient was unable to visually distinguish the compliant from the noncompliant socket, and strongly stated that the more compliant socket provided the greatest comfort.

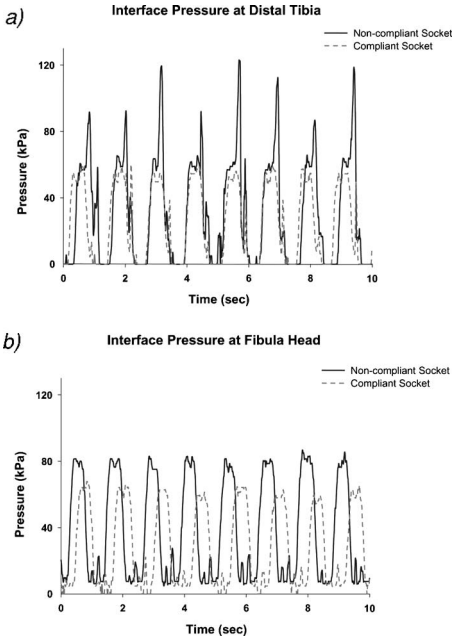

Fig. 7 (*a*) Interface contact pressure measured at the distal tibia for both the noncompliant and most compliant sockets; (*b*) interface contact pressures at the fibula head. (Only the first 10 seconds of data are shown.)

Discussion

The goal of this work was to develop a strategy to design and implement orthogonally compliant features in SLS-produced transtibial prosthetic sockets to reduce residual limb-prosthesis contact pressure. High residual limb-socket contact pressures are the leading cause of pain and discomfort and can greatly hinder patient mobility [5,6]. The pressure measurements showed that we were successful in achieving this goal. The compliant features reduced the average and peak pressures by 22% and 45% at the distal tibia, respectively, and 19% and 23% at the fibula head, respectively. Also, subjective patient feedback indicated the more compliant socket was much more comfortable than the noncompliant one. Thus, although these results were from a single case study, the data suggest such compliant features hold great promise for improving the functional performance of prosthetic sockets. Future work will be directed at testing compliant sockets on a large population of transtibial amputees.

The topology optimization results showed that slight changes in topologies can produce considerable changes in the resulting com-

Table 1 Peak and average interface contact pressure at the distal tibia and fibula head during single leg support averaged over 40 step cycles. Socket B was 25% more compliant than socket A.

	Pressure Measurement Results from Case Study		
	Noncompliant Socket	Compliant Socket A	Compliant Socket B
Average pressure at distal tibia during single support	67.51±17.23 kPa	58.47±6.13 kPa	52.67±3.28 kPa
Average peak pressure at distal tibia	103.35±15.59 kPa	67.83±8.11 kPa	57.01±1.87 kPa
Average pressure at fibula head during single support	73.85±9.03 kPa	62.86±5.37 kPa	59.50±4.06 kPa
Average peak pressure at fibula head	82.74±1.84 kPa	70.59±1.56 kPa	63.60±2.63 kPa

pliance (Fig. 6). Fine-tuning the compliance can also be achieved by slightly changing the thickness of the structures involved, such as the back protective wall and the inner compliant membrane [Fig. 4(*b*)]. However, precisely predicting the actual contact pressure reduction of the compliant feature during the design phase of the socket is a much more complex problem, which includes not only the geometry of the resulting socket but the geometry and material properties of the residual limb and its underlying tissues. A potential solution to address this problem is to use a validated FEM model and analysis to predict *a priori* the resulting deflections for a given design [15]. This is an area of ongoing research.

One potential limitation of compliant features is the uncertainty of their long-term structural reliability under the dynamic, cyclical loads that occur during normal walking. Thus, a future consideration should be socket fatigue, which can be included as a design parameter. We are also currently testing other SLS materials with higher fatigue strength such as Nylon 11.

Another approach for providing compliance in sockets not explored in the present study is varying the porosity within the SLS fabrication. As described in the Methods section (see *Topology Optimization of Features for Controlled Compliance*), the variables for the topology optimization are the element densities in the design domain. The final target value for each element density is either the minimum value (no material) or one (presence of material). However, since it may be possible to change the density of the part by introducing porosity during SLS fabrication, other target values for element density might be acceptable in the topology optimization, leading to more alternatives for compliant structures.

Although the present work focuses on providing compliant features to PTB sockets, the same methods can be applied to integrate compliant features into other socket designs, such as total surface bearing (TSB) sockets. TSB socket designs are challenging since they rely on a vacuum fit of the socket on the residual limb. However, the only adaptation to the present framework would be to reposition the holes that are located on the protective wall of the compliant features [Fig. 4(*a*)]. Those holes serve to facilitate the removal of unsintered powder from the cavities formed by the compliant features, and they could easily be redesigned to pass through the walls of the compliant feature leading towards the inner surface of the socket, thus preserving an intact boundary between the limb-socket interface region and the outside of the socket. This would allow negative pressure to be developed at the interface, thus facilitating the vacuum fit between the socket and residual limb.

The long-term goal of this research is to establish a rapid, customized fabrication process for prosthetic sockets that would provide a practicing prosthetist a framework to define a compliant socket and transmit electronic data to an SLS service bureau to manufacture the socket. The completed socket would then be delivered to the prosthetist for patient fitting in a matter of days rather than the current practice of weeks or months. This process will require a targeted CAD environment that allows a prosthetist to incorporate compliant features, possibly from a library of features, into the socket design without requiring intensive CAD training. The prosthetist would then be able to analyze various designs and receive valuable feedback on their performance from patients. Development of this framework is the focus of ongoing research.

Acknowledgments

This research was supported by the VA Research and Development Service, Grant No. A2755R. We also acknowledge support from CNPq for M.C.F.

References

[1] Howell, L. L., 2001, *Compliant Mechanisms*, John Wiley & Sons, New York.
[2] Rogers, W. E., Crawford, R. H., Beaman, J. J., and Walsh, N. E., 1991, "Fabrication of Prosthetic Sockets by Selective Laser Sintering," 1991 Solid Freeform Fabrication Symposium Proceedings, Marcus, H. L., Beaman, J. J., Barlow, J. W., Bourell, D. L., and Crawford, R. H., eds., Austin, TX, 1991, pp. 158–163.
[3] Walsh, N. E., Lancaster, J. L., Faulkner, V. W., and Rogers, W. E., 1989, "A Computerized System to Manufacture Prostheses for Amputees in Developing Countries," Prosthet. Orthot Int., **1**, No. 3, pp. 165–181.
[4] Faustini, M., Modeling and Fabrication of Prosthetic Sockets using Selective Laser Sintering, Doctoral dissertation, The University of Texas at Austin, 2004.
[5] Mak, A. F. T., Zhang, M., and Boone, D. A., 2001, "State-of-the-Art Research in Lower-Limb Prosthetic Biomechanics-Socket Interface," J. Rehabil. Res. Dev., **38**, No. 2, pp. 161–173.
[6] Legro, M. W., Reiber, G., del Aguila, M., Ajax, M. J., Boone, D. A., Larsen, J. A., Smith, D. G., and Sangeorzan, B., 1999, "Issues of Importance Reported by Persons With Lower Limb Amputations and Prostheses," J. Rehabil. Res. Dev., **36**, No. 3, pp. 155–163.
[7] Buis, A. W. P., and Convery, P., 1998, "Conventional Patellar-Tendon-Bearing (PTB) Socket/Stump Interface Dynamic Pressure Distributions Recorded During the Prosthetic Stance Phase of Gait of a Trans-Tibial Amputee," Prosthet. Orthot Int., **22**, pp. 193–198.
[8] Bendsoe, M. P., and Kikuchi, N., 1993, "Generating Optimal Topologies in Structural Design Using a Homogenization Method," Comput. Methods Appl. Mech. Eng., **71**, pp. 197–224.
[9] Nishiwaki, S., Frecker, M., Min, S., and Kikuchi, N., 1998, "Topology Optimization of Compliant Mechanisms Using the Homogenization Method," Int. J. Numer. Methods Eng., **42**, pp. 535–559.
[10] Suzuki, K., and Kikuchi, N., 1991, "A Homogenization Method for Shape and Topology Optimization," Comput. Methods Appl. Mech. Eng., **93**, pp. 291–318.
[11] Bendsoe, M. P., and Sigmund, O., 1999, "Material Interpolation Schemes in Topology Optimization," Arch. Appl. Mech., **69**, pp. 635–657.
[12] Sigmund, O., and Peterson, J., 1998, "Numerical Instabilities in Topology Optimization: A Survey on Procedures Dealing With Checkerboards, Mesh-Dependencies and a Local Minima," Struct. Multidiscip. Optim., **16**, pp. 68–75.
[13] Sigmund, O., 2001, "A 99 Line Topology Optimization Code Written in Matlab," Struct. Multidiscip. Optim., **21**, No. 2, pp. 120–127.
[14] Svanberg, K., 1987, "The Method of Moving Asymptotes—A New Method for Structural Optimization," Int. J. Numer. Methods Eng., **24**, pp. 359–373.
[15] Faustini, M. C., Neptune, R. R., and Crawford, R. H., 2005, "The Quasi-Static Response of Compliant Prosthetic Sockets for Transtibial Amputees Using Finite Element Methods," Med. Eng. Phys. (in press).